Supporting Information for "Synchronous emplacement of anorthosite xenoliths, the Beaver River diabase, and the Greenstone Flow"

Field observations on sampled Beaver River diabase and anorthosite xenoliths

The measured dimensions of each anorthosite xenolith sampled during the fieldwork of this study are summarized in Table DR1. The estimated distance from each anorthosite site to the closest diabase site are also show in the table.

Table DR1. Summary of anorthosite xenolith dimensions and their approximate distance between each anorthosite site and the closest diabase site.

Anorthosite site	Xenolith dimension (m)	Closest diabase site	Distance from anorthosite site to closest diabase site (m)
AX1	3.1 X 1.3	BD1	<5
AX2	4 X 15 X 30	BD1	<5
AX3	100 X 30	BD2	200
AX4	20 X 10	BD2	50
AX5	0.5 X 0.45	BD2	20
AX6	0.7 X 0.6	BD2	20
AX7	0.8 X 0.5	BD2	20
AX8	0.4 X 0.25	BD2	20
AX9	0.3 X 0.6	BD2	20
AX10	0.47 X 0.47	BD2	20
AX11	120 X 30	BD3	150
AX12	31 X 5	BD4	32
AX13	36 X 8	BD3	30
AX14	10 X 3	BD4	150
AX15	5.8 X 5.5	BD5	<5
AX16	27.5 X 5	BD5	25
AX17	4.2 X 2	BD5	<5
AX18	15.6 X 3	BD5	<5
AX19	7.5 X 2.9	BD6	9
AX20	8.1 X 6.5	BD7	<5
AX21	3.2 X 1.2	BD7	300
AX22	5 X 12 X 10	BD10	<10

Beaver River diabase structural correction

Structural measurements were obtained from the published geologic maps of the study area. We calculated the mean directions from the combined volcanic bedding measurements from the Schroeder-Lutsen basalt and igneous layering measurements from the Beaver River diabase and constructed two sets of tilt correction data for the paleomagnetic sites in the southern and eastern Beaver Bay Complex Boerboom (2004); Boerboom and Green (2006); Boerboom et al. (2006, 2007); Miller et al. (2006). The mean dip angle for the two areas are very similar while the dip

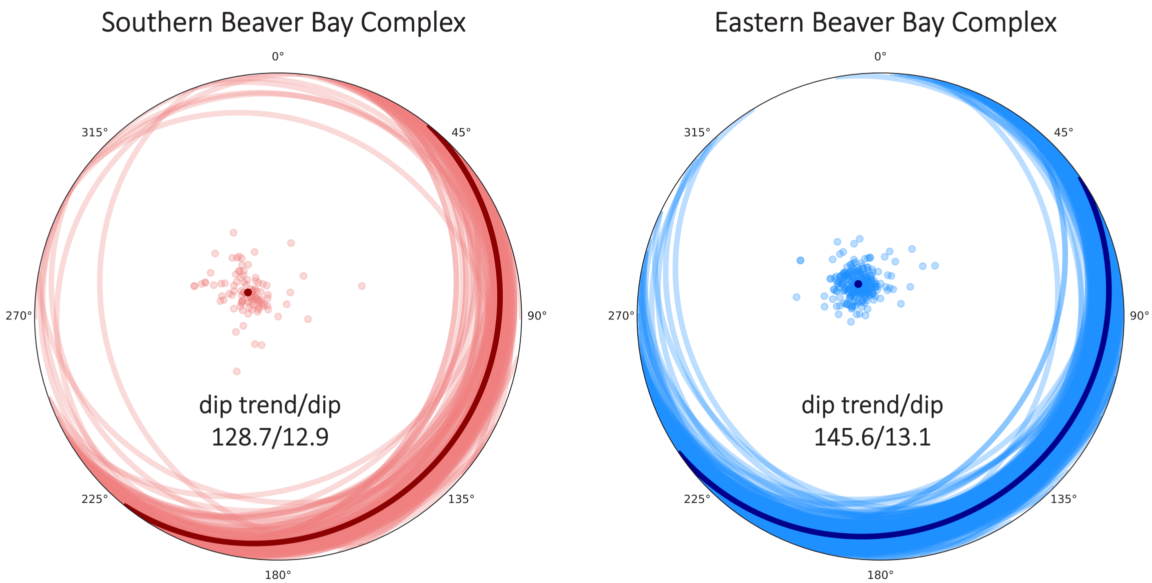

Figure SI1. Stereonet plots of the compiled structural orientation data to tilt correct the paleomagnetic directions obtained from the Beaver River diabase and the anorthosite xenoliths therein.

trends are different, with the southern Beaver Bay Complex showing a slightly more easterly trend than the eastern Beaver Bay Complex. This difference in dip trend reflects the overall arcuate shape of the Beaver Bay Complex intrusions along the shore of Lake Superior.

ID-TIMS U-Pb zircon geochronology methods

U-Pb dates were obtained by chemical abrasion isotope dilution thermal ionization mass spectrometry (ID-TIMS) in the Boise State University (BSU) Isotope Geology Laboratory (Table DR2; Fig. SI3). Chemical abrasion of single zircon grains was modified after Mattinson (2005). Zircons were separated from rocks using standard techniques, annealed in a muffle furnace at 900°C for 60 hours in quartz crucibles.

Individual zircons were removed from grain mounts and chemically abraded. Chemical abrasion was carried out by transferring zircons to 3 ml Teflon Perfluoroalkoxy alkane (PFA) beakers in which they were rinsed in 3.5 M HNO_3 and ultrapure H_2O prior to loading into 300 μl Teflon PFA microcapsules. Fifteen microcapsules were placed in a large-capacity Parr vessel and the zircon partially dissolved in 120 μl of 29 M HF for 12 hours at 190°C. Zircons were returned to 3 ml Teflon PFA beakers, HF was removed, and zircons were immersed in 3.5 M HNO_3, ultrasonically cleaned for an hour, and fluxed on a hotplate at 80Â°C for an hour. The HNO_3 was removed and zircon was rinsed twice in ultrapure H2O before being reloaded into the 300 μl Teflon PFA microcapsules (rinsed and fluxed in 6 M HCl during sonication and washing of the zircons) and spiked with the ^{233}U-^{235}U-^{205}Pb BSU tracer solution (BSU1B). Zircons were dissolved in Parr vessels in 120 μl of 29 M HF at 220°C for 48 hours, dried to fluorides, and re-dissolved in 6 M HCl at 180°C overnight. Pb and U were separated from the zircon matrix using an HCl-based anion-exchange chromatographic procedure (Krogh, 1973), eluted together and dried with 2 μl of 0.05 N H_3PO_4.

Pb and U were loaded on a single outgassed Re filament in 5 μl of a silica-gel/phosphoric acid mixture (Gerstenberger and Haase, 1997), and Pb and U isotopic measurements made on a GV Isoprobe-T multicollector thermal ionization mass spectrometer equipped with an ion-counting Daly detector. Pb isotopes were measured by peak-jumping all isotopes on the Daly detector for 190 cycles with a mass bias correction of 0.16 $\pm$ 0.03%/a.m.u. (1σ). Transitory isobaric interferences due to high-molecular weight organics, particularly on ^{204}Pb and ^{207}Pb, disappeared within 30-45 cycles, while ionization efficiency averaged 104 cps/pg of each Pb isotope. Linearity (to $\geq$1.4 x 10^6 cps) and the associated deadtime correction of the Daly detector were determined by analysis of NBS982. Uranium was analyzed as UO_2^+ ions in static Faraday mode on 10^{12} ohm resistors for up to 300 cycles, and corrected for isobaric interference of $^{233}U^{18}O^{16}O$ on $^{235}U^{16}O^{16}O$ with an $^{18}O/^{16}O$ of 0.00206. Ionization efficiency averaged 20 mV/ng of each U isotope. U mass fractionation was corrected using the $^{233}U/^{235}U$ ratio of the BSU1B tracer.

Table DR2. Zircon chemical abrasion IDTIMS U-Pb isotopic data

	Compositional Parameters						Radiogenic Isotope Ratios									Isotopic Ages					
Sample (a)	$\frac{Th}{U}$ (b)	$^{206}Pb^*$ $\times10^{-13}$ mol (c)	mol % $^{206}Pb^*$ (c)	$\frac{Pb^*}{Pb_c}$ (c)	Pb_c (pg) (c)	$\frac{^{206}Pb}{^{204}Pb}$ (d)	$\frac{^{208}Pb}{^{206}Pb}$ (e)	$\frac{^{207}Pb}{^{206}Pb}$ (e)	% err (f)	$\frac{^{207}Pb}{^{235}U}$ (e)	% err (f)	$\frac{^{206}Pb}{^{238}U}$ (e)	% err (f)	corr. coef.	$\frac{^{207}Pb}{^{206}Pb}$ (g)	± (f)	$\frac{^{207}Pb}{^{235}U}$ (g)	± (f)	$\frac{^{206}Pb}{^{238}U}$ (g)	± (f)
MS99033 *Anorthosite xenolith in Beaver Bay Diabase* (Beaver Bay Complex)																				
z4	0.944	0.8673	0.9977	144	0.17	7696	0.286	0.0759659	0.066	1.93250	0.118	0.184584	0.077	0.856	1093.27	1.31	1092.41	0.79	**1091.97**	**0.77**
z8	1.010	6.9857	0.9997	1133	0.18	59449	0.306	0.0759607	0.040	1.93235	0.083	0.184583	0.046	0.974	1093.13	0.81	1092.35	0.56	**1091.96**	**0.46**
z1	2.435	6.7175	0.9985	309	0.81	12367	0.738	0.0759449	0.047	1.93191	0.087	0.184579	0.046	0.948	1092.72	0.93	1092.20	0.59	**1091.94**	**0.46**
z7	1.008	1.4490	0.9986	239	0.17	12587	0.305	0.0759289	0.056	1.93127	0.098	0.184557	0.055	0.886	1092.30	1.11	1091.98	0.66	**1091.82**	**0.55**
z3	1.863	3.3407	0.9992	519	0.22	22932	0.565	0.0759415	0.044	1.93139	0.086	0.184538	0.046	0.950	1092.63	0.89	1092.02	0.58	**1091.72**	**0.47**
z6	0.978	0.8594	0.9978	154	0.16	8164	0.296	0.0759062	0.059	1.93015	0.101	0.184504	0.055	0.878	1091.70	1.19	1091.59	0.68	**1091.54**	**0.55**
z5	0.971	1.3031	0.9983	196	0.19	10381	0.294	0.0759732	0.056	1.93131	0.095	0.184453	0.050	0.891	1093.46	1.12	1091.99	0.64	1091.26	0.50
z2	0.909	1.7688	0.9985	229	0.22	12318	0.276	0.0759373	0.053	1.93029	0.093	0.184443	0.049	0.910	1092.52	1.06	1091.64	0.62	1091.20	0.49
												weighted mean 206Pb/238U age = 1091.83 ± 0.21 (0.37) [1.15] Ma (2s); MSWD = 0.41 (n=6)								

(a) z1, z2 etc. are labels for single zircon fragments annealed and chemically abraded after Mattinson (2005); bold indicates analyses used in weighted mean calculations.
(b) Model Th/U ratio iteratively calculated from the radiogenic 208Pb/206Pb ratio and 206Pb/238U age.
(c) Pb* and Pbc represent radiogenic and common Pb, respectively; mol % $^{206}Pb^*$ with respect to radiogenic, blank and initial common Pb.
(d) Measured ratio corrected for spike and fractionation only. Fractionation estimated at 0.18 (Daly) or 0.10 (Faraday) ± 0.02 %/a.m.u. based on analysis of NBS-981 & 982.
(e) Corrected for fractionation, spike, and common Pb; all common Pb was assumed to be procedural blank: 206Pb/204Pb = 18.60 ± 0.72%; 207Pb/204Pb = 15.69 ± 0.62%; 208Pb/204Pb = 38.51 ± 0.74% (all uncertainties 1-sigma). Isotope dilution measurements made with the ET535 spike (Condon et al., 2015).
(f) Errors are 2-sigma, propagated using the algorithms of Schmitz and Schoene (2007).
(g) Calculations are based on the decay constants of Jaffey et al. (1971). All ratios and ages corrected for initial 230Th/238U disequilibrium with Th/U [magma] = 3.

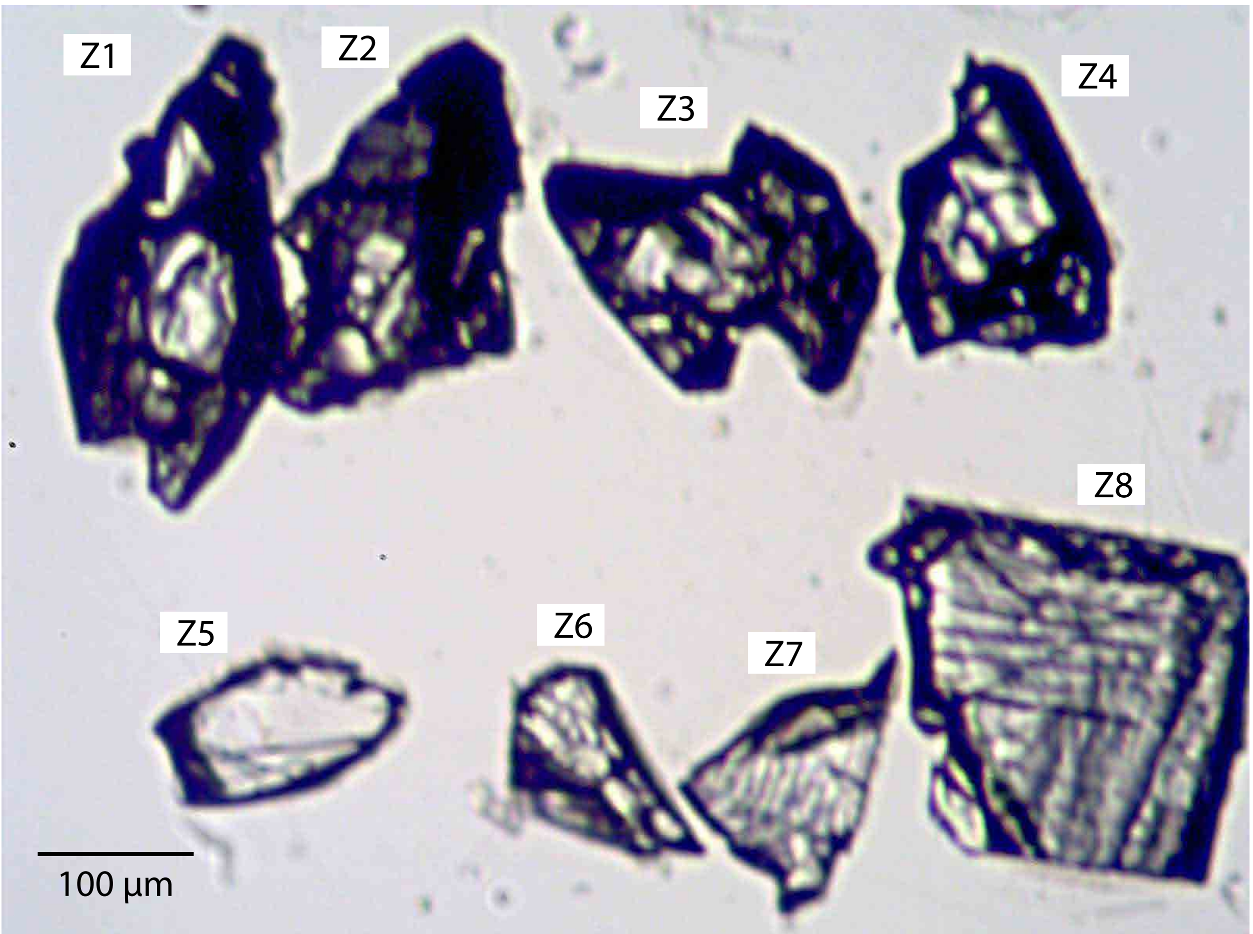

Figure SI2. Image of individual zircons from geochronology sample MS99033. Zircons (z1-z4) are subhedral to anhedral crystals and (z5-z8) are platy fragments.

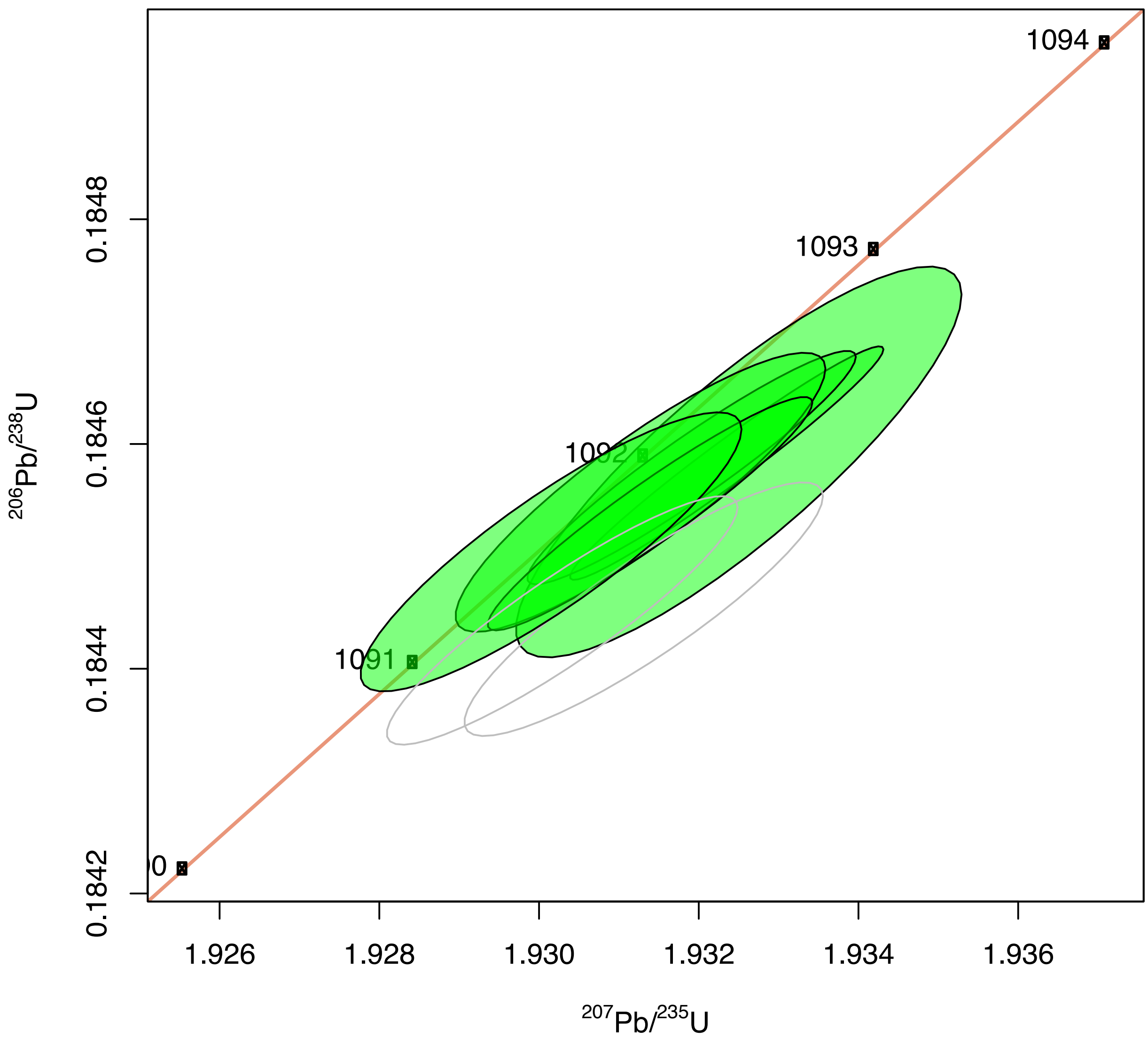

Figure SI3. U-Pb concordia plots for the new zircon dates from anorthosite xenoliths AX16, geochronology sample name MS99033. The ellipses represent 2σ analytical uncertainty on individual zircon dates. Green filled ellipses are analyses included in the $^{2}06Pb/^{2}38U$ weighted mean dates while the grey ellipses are those that were excluded.

References

Boerboom, T. J. (2004).M-147 Bedrock geology of the Split Rock Point quadrangle, Lake County, Minnesota(Tech. Rep.). Minnesota Geological Survey.

Boerboom, T. J., & Green, J. C.(2006). M-170 Bedrock geology of the Schroeder quadrangle, Cook County, Minnesota(Tech. Rep.). Minnesota Geological Survey.

Boerboom, T. J., Green, J. C., Albers, P., & Miller, J., J.D. (2006).M-171 bedrock geology of the tofte quadrangle, cook county, minnesota(Tech. Rep.).Minnesota Geological Survey.

Boerboom, T. J., Green, J., & Albers, P. (2007).M-174 Bedrock geology of the Lutsen quadrangle, Cook County, Minnesota(Tech. Rep.). Minnesota Geological Survey.

Gerstenberger, H. and Haase, G., 1997, A highly effective emitter substance for mass spectrometric Pb isotope ratio determinations: Chemical Geology, vol. 136, pp. 309–312.

Hiess, J., Condon, D. J., McLean, N., and Noble, S. R., 2012, ^{238}U/^{235}U systematics in terrestrial uranium-bearing minerals: Science, vol. 335, pp. 1610–1614, doi:10.1126/science.1215507.

Krogh, T., 1973, A low contamination method for the hydrothermal decomposition of zircon and extraction of U and Pb for isotopic age determinations: Geochimica Cosmochimicha Acta, vol. 37, pp. 485–494, doi:10.1016/0016-7037(73)90213-5.

Ludwig, K. R., 2003, Isoplot 3.0. a geochronological toolkit for Microsoft Excel: Tech. rep., Berkeley Geochronology Center.

Mattinson, J. M., 2005, Zircon U/Pb chemical abrasion (CA-TIMS) method: Combined annealing and multi-step partial dissolution analysis for improved precision and accuracy of zircon ages: Chemical Geology, vol. 220, pp. 47–66, doi:10.1016/j.chemgeo.2005.03.011.

Miller, J., J.D., Severson, M. J., Chandler, V. W., & Peterson, D. M. (2001).M-119651Geologic map of the Duluth Complex and related rocks, northeastern Minnesota652(Tech. Rep.). Minnesota Geological Survey.

Schmitz, M. D. and Schoene, B., 2007, Derivation of isotope ratios, errors, and error correlations for U-Pb geochronology using ^{205}Pb-^{235}U-(^{233}U)-spiked isotope dilution thermal ionization mass spectrometric data: Geochem. Geophys. Geosyst., vol. 8, p. Q08,006, doi:10.1029/2006GC001492.